Challenge and Innovations of Carburized gears for Remanufacturing

Tomohisa Kanazawa[1]*§, Masao Hayakawa[2*], Akinori Kondo[1], Dan Vinas[1], Mitsuhiro Yoshimoto[1], Masakazu Nakasako[3]

[1]Remanufacturing Div., Hitachi Construction Machinery Co., Ltd, Tsuchiura city Kandatsu 650, Japan.
[2]National Institute for Materials Science (NIMS), Tsukuba city Sengen 1-2-1, Japan.
[3]National Institute of Technology, Kure College, Kure city Aga minami 2-2-11, Japan.

*These authors contributed equally to this work
[§]Corresponding author

Email addresses: t.kanaazawa.zn@hitachi-kenki.com

Abstract

In recent years, the mass consumption of resources and climate change have become global social issues. Remanufacturing, which is categorized, is attracting attention in various industries because it has high economic efficiency due to the resource saving effect by reusing inner parts, low manufacturing cost, and new employment creation.

The remanufacturing industry of construction and mining equipment has a relatively large market size as regular maintenance and parts are larger and more expensive than other industries components. Among various remanufactured components, carburized gears and bearings, which are often used in prime movers and reduction gears, are one of the parts that are prone to wear and surface damage under high load conditions.

In this theme, we will introduce the development contents of non-destructive testing and functional recovery technology. that specializes in remanufacturing for this issue.

Introduction

More than 250 years have passed since the Industrial Revolution (late 18th century), and currently, human-made mass, especially from manufacturing units and construction, exceeds all living biomass [1]. Under these circumstances, Industries, governments, and businesses have contributed to achieve a sustainable society. Remanufacturing, the goods from which have been categorized as “reused or recycled industries,” is effective in saving resources through the reuse of subparts and is more economically efficient than other means of recycling resources. Therefore, remanufacturing is used as a major means of achieving economic and environmental benefits [2].

Mining machines as one model of heavy duty off-load equipment (HDOR) are required to run for about 20 hours per day, 365 days per year (equivalent to about 5,000 to 6,000 hours per year) for about 10 years, but they must be taken out of service for regular overhauls. Long out-of-service time is a factor that significantly affects urban infrastructure development and resource mining operations. The crucial need for construction machinery manufacturers to bring machines back into service as quickly as possible creates a strong demand for remanufactured parts in the field of construction and mining machinery [3]. The use of remanufactured parts contributes significantly to reducing the out-of-service time and maintenance cost of machines.

The major remanufactured parts used of HDOR include hydraulic cylinders, hydraulic pumps, transmissions and reducers. Gear parts commonly used in reducers are expensive and are scrapped at high rates. For this reason, it is necessary that in the remanufacturing process, gear parts be removed from components that have been used for a certain period of time, assessed for integrity (= reusability) and then reused where possible. In the current remanufacturing process, a worker visually inspects only the gear parts that have been subjected to relatively low loads for defects such as gear surface pitting, takes dimensional measurements, and determines whether or not reuse is possible. Typical forms of damage are gear surface pitting and wear. About 30% of gears without pitting are scrapped. To be able to reuse these parts, it is necessary to establish a science-based damage assessment method based on non-destructive testing (NDT). More important issue is the establishment of functional recovery technology based on knowledge obtained through NDT development.

Previous some studies of NDT evaluate mechanical properties and structural changes after elemental tests, and it is difficult to apply them to the evaluation of parts recovered from operating machines whose load history is unknown [3-6].

On the other hand, in terms of function restoration technology, there are research studies on overlaying using additive manufacturing technology. However, there are no research themes on remanufacturing based on functional recovery of changes in the inner surface of alloy that are not accompanied by defects [7-9].

In this study, with the aim of assessing damage to carburized gears, we investigated changes in the microstructure and mechanical properties of metals by comparing gears, carburized parts collected from a machine in operation, and element-tested specimens [10]. We analyzed the relationship between these factors and propose a method for assessing damage to carburized gears, including those with an unknown operating history. Moreover, in our research, we have realized the mechanical and structural function recovery of the gear surface layer only by laser hardening (LH) treatment, which is one of the simple and inexpensive heat treatment [11].

Results and Discussion

Evaluation of surface and section structures

Figure 1 show as the roller pitching testing and gear. Fig.1(a) and (b), (c) were not found the clearly cracks. In the meanwhile, Fig.7(b) of surface pressure 3.7 GPa (2.6×105 cycles) is clearly visible the crack on the friction surface. The surface of (e) become evident the pitching damage. The surface of before operating gear (f) is same configuration as surface of Fig.7(a), the gear surface of after operating is not also became clearly evident the crack or pitching. Therefore, it is not able to capture the damage behaviour change only surface configuration.

Figure 2 shows an SEM image of surface section. In the before testing specimen (a), γR (white arrow) with a single contrast is observed in the martensite phase. In the gear (b) after operating, the fine γR is observed, but coarse γR with a width of 2 μm or more disappears. On the other hand, in the pitching damage specimen (c), the fine γR disappeared.

Damage evaluation method

As shown in Fig. 3, in the undamaged region A, the σX ratio tends to increase as the γR ratio decreases. In this region, no microcracks were formed even from the state of the surface layer (Fig. 1 (b), (c), (g)).

In the damaged area B, the γR ratio and the σX ratio decrease over the entire surface even on the sliding surface other than the pitching portion as shown in fig. 1(d), and the microscopic changes due to sliding fatigue are also captured. Therefore, even for gears that are difficult to judge by visual judgment or simple evaluation of dimensional measurement, it is possible to judge whether or not they can be reused by the numerical values of the γR ratio and the σX ratio.

Fatigue lives before and after LH

The results of fatigue testing before and after LH are presented in Fig. 4. In addition, the state at each step of LH treatment is shown. The fatigue life of the steel (up to the point of pitching) without LH was 1.7×10^6 cycles (Specimen 1). The percentage in the figure represents the ratio of the number of interrupted-test cycles to the number of cycles to failure. Interrupted-test specimens (Specimens 2–5) were subjected to LH and tested again. The fatigue lives of the steel (up to the point of failure) were 6.5×10^6 cycles (3.8 times greater than that of the steel without LH; 15% interrupted), 5.5×10^6 cycles (3.2 times greater; 50% interrupted), 4.5×10^6 cycles (2.7 times greater; 75% interrupted), and 2.3×10^6 cycles (1.3 times greater; 85% interrupted) for Specimens 2,3,4, and 5, respectively. As the rate of interruption increased, the lifetime after LH decreased. LH was only slightly effective in increasing the fatigue life of Specimen 5.

Fatigue damage, microstructure, and XRD pattern

Figures 5(a)–5(c) show the friction-fatigue damage, microstructure of the cross-section of the surface layer, and ratio of the Debye ring formed by the cos α method to γR, respectively.

From Fig. 5(a), the 50%-interrupted-test specimen in Step 2 exhibited 2-mm-wide friction marks but had no cracks. In Step 3, after LH, the friction marks remained, but a 4-mm-wide laser-hardened region was observed. The pitching of specimens in Step 4 (after LH) and Step 5 (before LH) was formed.

The microstructure of the cross-section of the surface layer before testing (Step 1) in Fig. 5(b) shows γR with a flat contrast of approximately 1 μm, containing no carbide in the lath-martensite phase to align with a stripe lath parallel.

In the 50%-interrupted-test specimen (Step 2), most of the γR was depleted. In Step 3, after LH, γR formed again in the lath martensite. In Step 4, after failure, γR was almost transformed into martensite.

In Fig.5(c), there are two Debye rings, the inner ring (indicated by the black arrow) corresponds to body-centered cubic symmetry (martensite phase), and the outer ring corresponds to face-centered cubic (γR). The γR ratio can be obtained from the intensity ratio of the two rings.

In this fig.5, summarizes the XRD measurement and surface hardness results for each step. The intensity of the Debye rings in Step 3 was higher (γR of 28±7%) after LH than that in Step 1(γR of 18±1%) but lower in Steps 2 (γR of 10±1%), 4 (γR of 11±2%), and 5 (γR of 7±1%). This was in good agreement with the changes in the microstructure. The γR ratio showed changes similar to those in the Debye rings.

Hardness was Hv707 near the surface layer due to the carburizing treatment in Step 1, with a slight further hardening to Hv713 in Step 2 due to sliding fatigue. In Step 3, it rises to about Hv800 as a result of LH processing. In the surface layer condition of Steps 4 and 5, where pitching damage eventually occurred, Hv638 and 682 and a softening tendency were shown.

Figures 6 show the grains of prior γ with and without LH, SEM microstructure images. The grains with LH were 5 μm (Step 3) in size, considerably smaller than those without LH, which were 10 μm (Step 1), as can be observed from these microstructures.

Conclusions

For remanufacturing NDT using XRD method, the visual evaluation and dimensional measurement, a database (DB) that systematically summarizes the results of this method is required to improve the reliability of damage evaluation. Based on the DB, it is important to use the region where the γR ratio and σx ratio decrease for the surface layer of carburized parts as the evaluation criteria for reusability.

LH treatment for remanufacturing, which rapidly heats and cools friction-fatigue damaged carburized surfaces, has enabled a drastic microstructural modification through the reinforcement of composite structures. Recovering the volume fraction of Rγ and refining the grain of prior γ significantly increased fatigue life beyond that before LH (new parts). Therefore, LH will be expected an effective remanufacturing technique for worn carburized parts.

As a result, the reuse rate of parts will increase, and the environmental burden will be reduced. According to some studies, the GWP of the reuse rate of gear parts was decreased by using remanufacturing or remanufacturing technology on the of mining parts [2,12]. Therefore, the technological aspect of remanufacturing is considered in order to satisfy the requirements of sustainable technology, which include strong environmental affinity.

Methods

Material

The material tested was ASTM4118 steel (0.2C, 0.8Mn, 0.22Si, 0.5Cr, 0.12Mo; mass%), which is commonly used for gear parts. It was formed into a cylinder as fig.7(a), normalized and carburized. The Vickers hardness was Hv350-400 inside the specimen and approximately Hv700 in the carburized layer. Additionally, the other specimen cut out of the gears collected from a machine in operation. No evident cracks were found in the surface of any of the gears collected from machines in operation as fig.7(b).

Friction fatigue test and evaluation step

The roller-pitching test was conducted as a friction fatigue test condition of table 1. The specimen consists of a driver and brake roller as fig.7(a). At the time of LH, the test was performed by dividing into each step under only one condition as shown in fig.8.

Laser hardening (LH)

Figure 9 is a schematic of the LH setup (Laser line Co., Ltd. LHF-50). A semiconductor-type laser was used that reached high output in the kW class, did not require the application of an absorbent.

X-ray diffraction (XRD)

For characterization of the specimens, the σX ratio and γR phase ratio in specimens (fatigue test piece and gears) before and after testing or operation was determined using a cosα method of X-ray diffractometer (30kV, 1.5mA, Cr Kα (λ=2.2910Å)). The

measurements were made before and after testing all specimens at the same position.

Authors' contributions

T.K. and M.H: Conceptualization. T.K: Methodology. T.K., M.H., D.V., and Y.T: Experiment. T.K. and H.M., D.V., A.K: Validation; T.K., M.H., and Y.T: Formal analysis. T.K: Investigation T.K. and M.Y: Resources. T.K., N.H., and M.Y: Data curation. T.K: Writing—original draft preparation. T.K., M.H., D.V., Y.T., N.N., and M.N: Writing—review and editing. T.K. M.H., N.N., D.V., A.K., M.Y., and M.N: Visualization. M.Y: supervision. T.K: Project administration. M.Y: Funding acquisition, M.Y. All authors have read and agreed to the published version of the manuscript.

Acknowledgements

We would like to thank M. Senzaki, E. Fukunishi, H. Fukumoto, M. Sugawara, S. Sakurai, Y. Wakabayashi, N. Hata and H. Akita Y. Tahara for useful discussions.

References

1. Elhacham E, Ben-Uri L, Grozovski J, Bar-On M.Y, Milo, R: Global human-made mass exceeds all living biomass, *Nature*. 2020, 588:442–444.
2. Kanazawa T, Matsumoto M, M, Yoshimoto, Tahara K: Environmental impact of remanufacturing mining machinery, *Sustainability*, 2022, 14:1-16.
3. Kanazawa T, Hayakawa M, Beltran D, Yoshimoto M, Saito K, Maruyama Y, Uchiyama M, Sasaki T: Nondestructive testing of friction-fatigued carburized martensitic steel, *Materials Transactions* 2021, 62:135-138.
4. Vashita M, Paul S: Correlation between full width at half maximum (FWHM) of XRD peak with residual stress on ground surface, *Philos. Mag* 2012, 92:4194-4204.
5. Miyazaki T, Sasaki T: X-ray stress measurement with two-dimensional detector based on Fourier analysis, *Int. Mater. Res* 2014, 105:922-927.
6. Li W, Ge J, Wu Y, Yin X, Chen G, Yuan X, Liu J, Yang W: An Electromagnetic Helmholtz-Coil Probe for Arbitrary Orientation Crack, *Material Transactions* 2017, 58:641-645.
7. Siavash H K, Joumi P, Jan. H: Additive manufacturing in the spare parts supply chain, *Comput. Ind*, 2014, 65:50–63.
8. Anas A S, Avanish K D: Recent trends in laser cladding and surface alloying, *Opt. Laser Technol* 2021, 134:1–20.
9. Ji Y D, Yan L L, Fang Y Li, Xue J R, Xing Y Z, Xiao X Qi: Research on the high temperature oxidation mechanism of Cr3C2-NiCrCoMo coating for surface remanufacturing, *JMR&T*. 2021, 10:565–579.
10. Kanazawa T, Hayakawa M, Yoshimoto M, Tahara Y, Hata N, Meguro S, Hiroto T, Matsushita Y, Sugawara M: Damage Evaluation of carburizing gear for remanufacturing, *Materials Transactions* 2022, 62:1660-1668.
11. Kanazawa T, Hayakawa M, Vinas D, Tahara Y, Hata N, Yoshimoto M: Sustainable Technology for Remanufacturing of Carburized Steels by Laser Hardening, *JMR&T*. 2023 24: 39-48.

12. Kanazawa T, Matsumoto M, Yoshimoto M, Sugawara M, Yoshimura A, Matsuno Y: Evaluation of environmental impact by applying remanufacturing technology for mining machinery parts, *J. LCA Soc. Jpn*. 2021, 17:124–135.

Figures

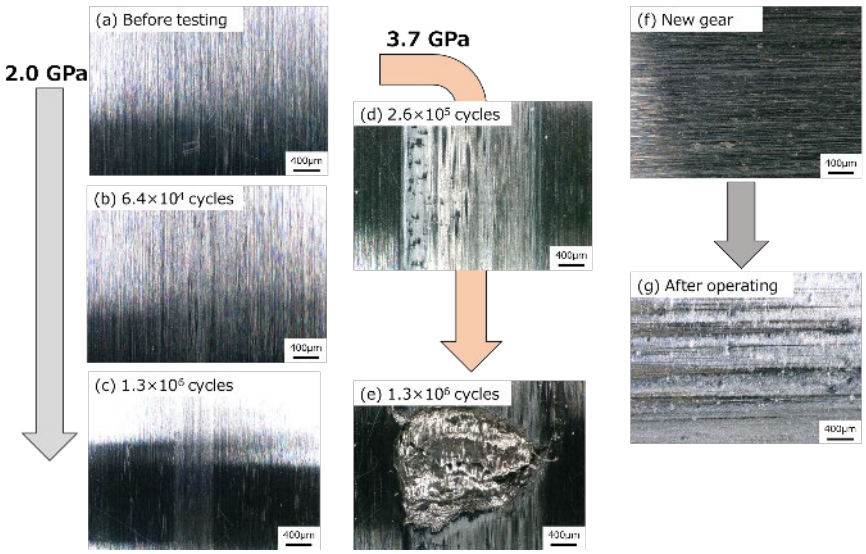

Figure 1 - Roller pitching test specimen and changes over time on the surface of the gear.

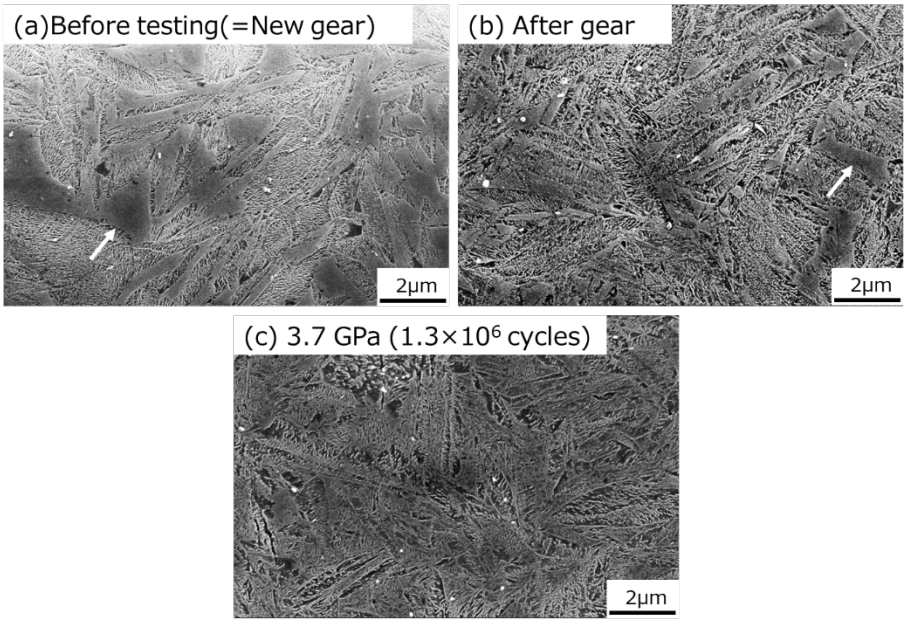

Figure 2 - SEM image of cross-sectional structure of carburizing treatment-martensite phase and retained austenite (white arrow).

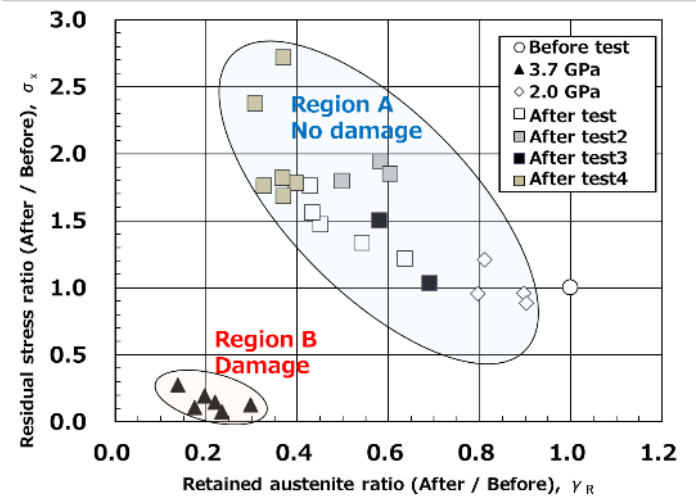

Figure 3 - Relationship between residual stress ratio and retained austenite ratio in damage evaluation.

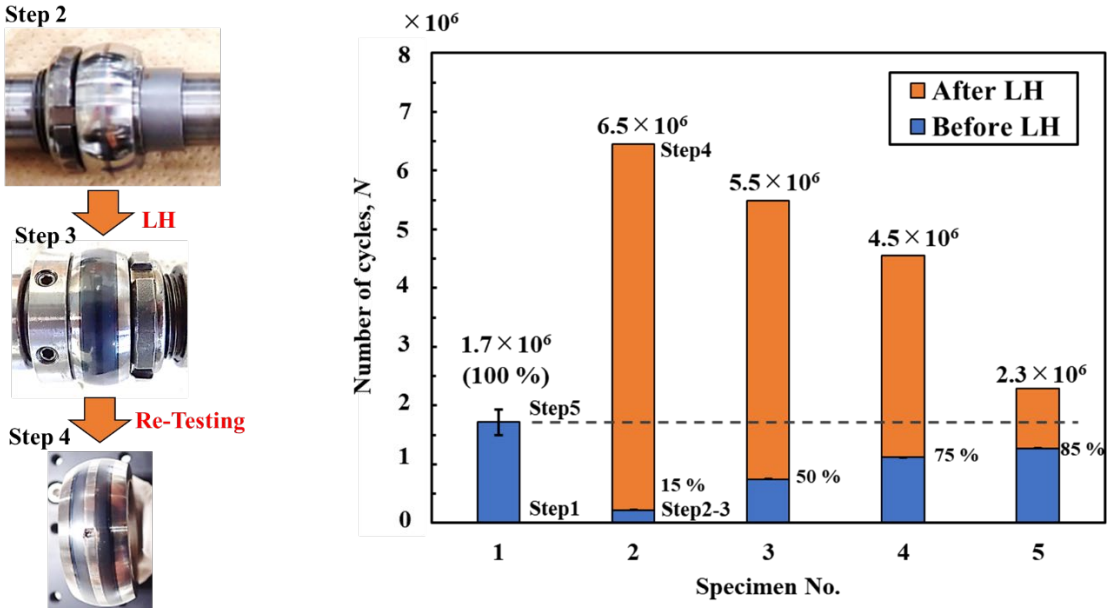

Figure 4 - Sliding fatigue life of each condition for roller-pitching testing.

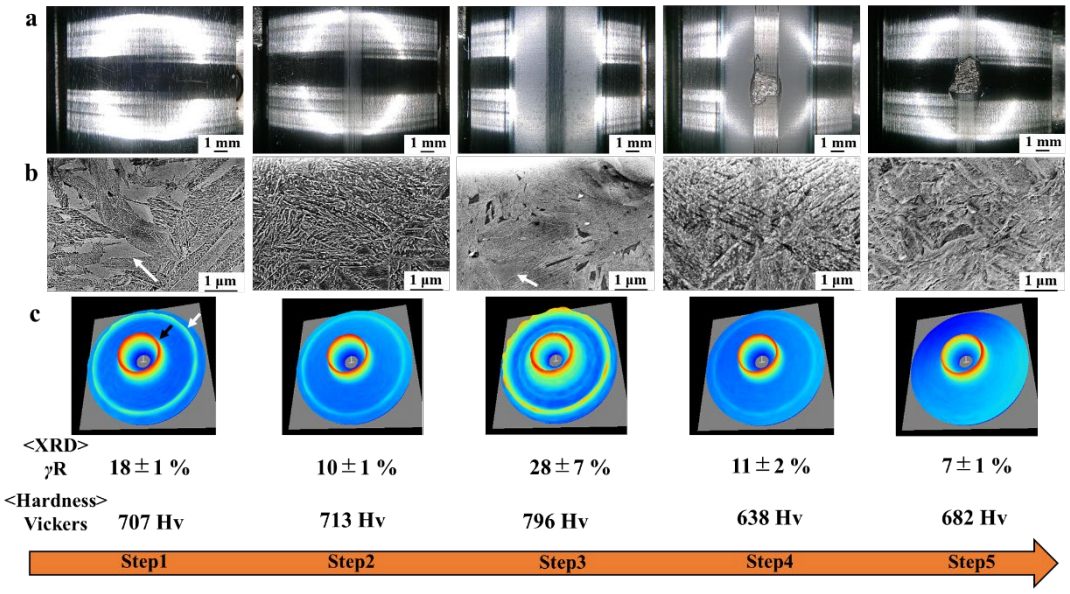

Figure 5 - Properties of specimen at different testing steps: (a) friction-fatigue surface; (b) SEM of cross-sections showing phase transformation and grain size of retained austenite; (c) XRD pattern Debye rings.

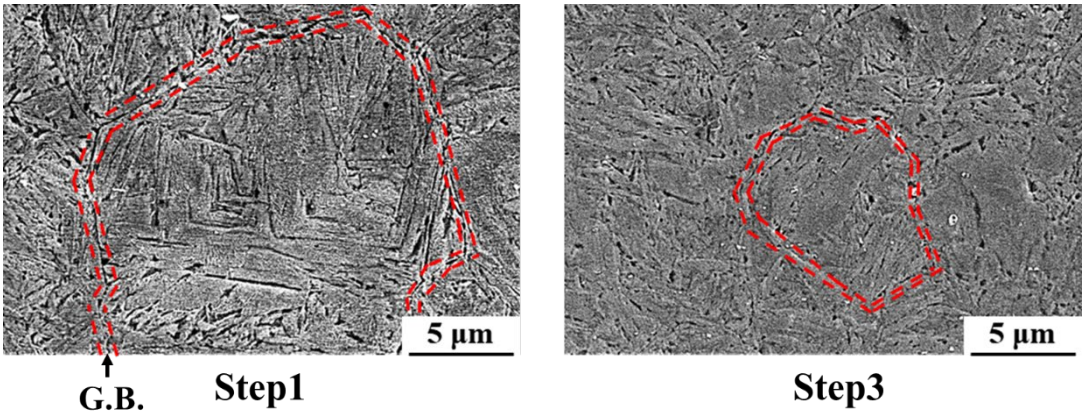

Figure 6 - SEM images of section structure: showing the particle-size change from 15–20 μm (Step 1) to ~5 μm (Step 3)

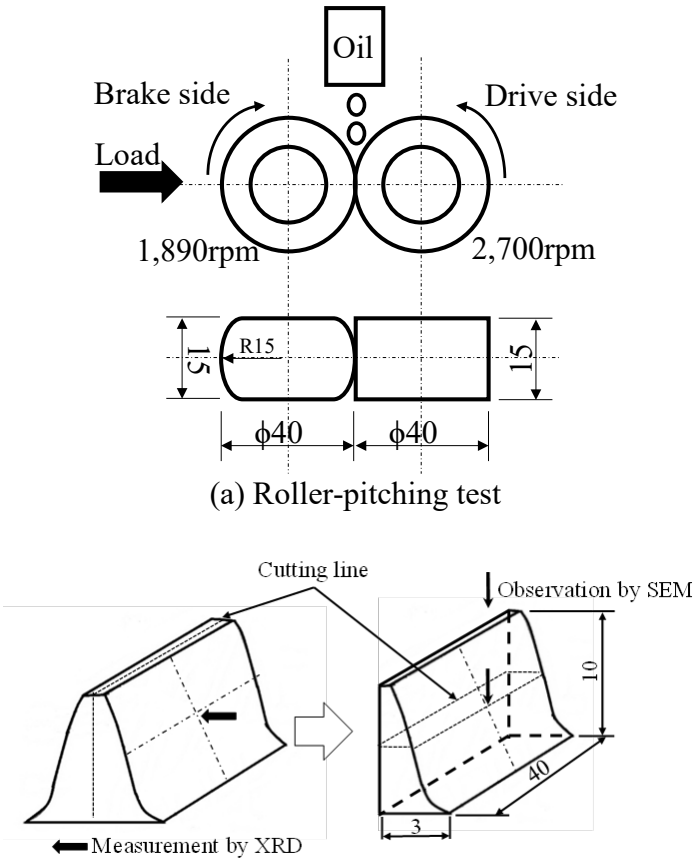

Figure 7 - Schematics of (a) roller-pitching test and (b) tooth surface of gear.

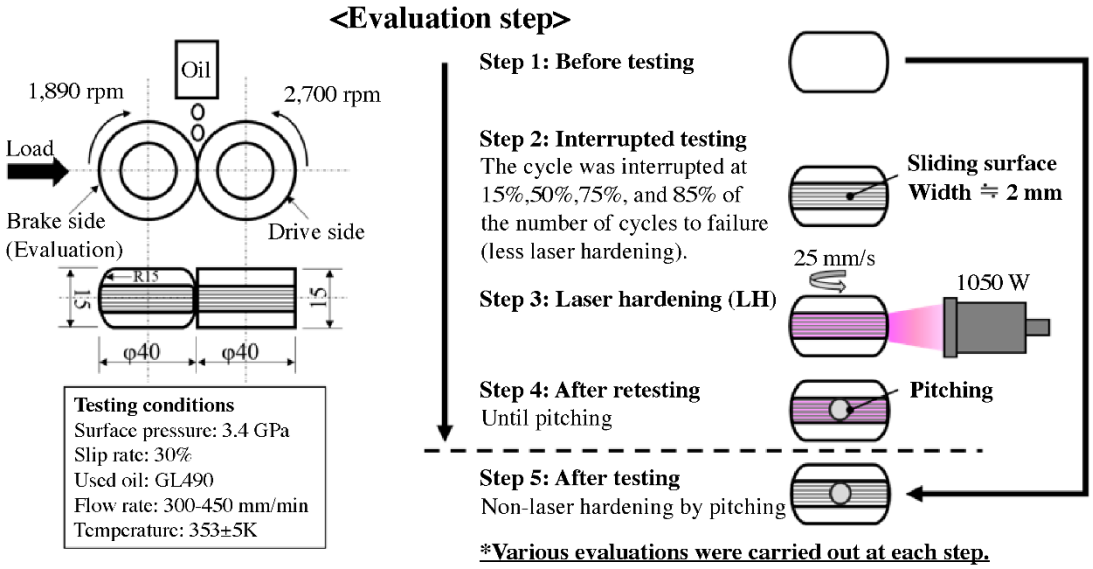

Figure 8 - Evaluation process of roller-pitching testing by LH.

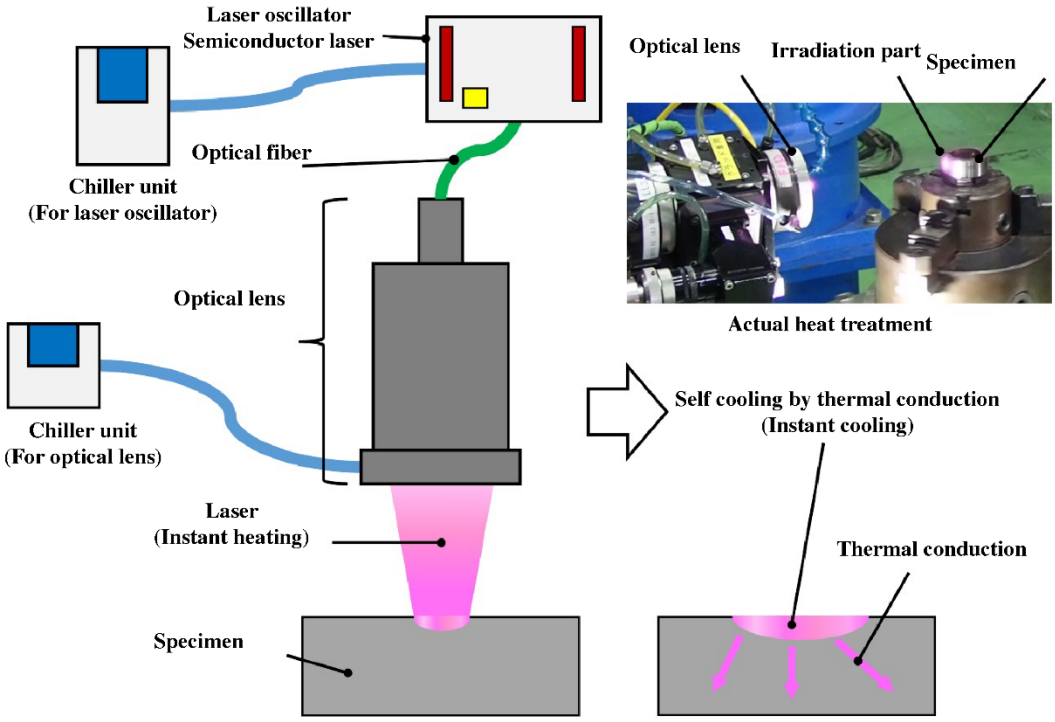

Figure 9 - Setup for laser hardening.

Tables

Table 1 - Testing conditions of roller–pitching

No.	Load, *P* / kN	Surface press, *SP* / GPa	Slip rate, *Sr* (%)	Oil	Flow rate, *Fr* / (ml/min)	Temp., *T* / ℃
1	1	2.0	30	GL490	300-450	80±5
2	6	3.7				